



# Cumulative quantum mechanics—Quantum-size effects for: nano-, angstrom- and femto-technologies

P. I. Vysikaylo

 Moscow Regional State University 105005 Moscow, Russian Federation; [filvys@yandex.ru](mailto:filvys@yandex.ru)

## ARTICLE INFO

Received: 16 April 2024  
Accepted: 20 May 2024  
Available online: xx 2024

doi: 10.59400/nc.vxix.1297

Copyright © 2024 Author(s).

*Nano Carbons* is published by Academic Publishing Pte. Ltd. This article is licensed under the Creative Commons Attribution License (CC BY 4.0).  
<http://creativecommons.org/licenses/by/4.0/>

**ABSTRACT:** The leading laboratories continue intensive research into the properties of nanocomposites—materials that have unique, both physical and chemical properties. Along with the discovery of new materials, new technologies are being developed and attempts are being made to create mathematical models capable of describing phenomena in hollow quantum resonators—quantum dots, lines, and other cumulative-dissipative 3D structures of nanometer dimensions. **New models make it possible to develop new materials, discover new patterns, and solve old fundamental problems in new ways.** The author has discovered and classified more than 32 polarization quantum-size effects. **We can explain all the quantum-size effects that we have discovered only by applying the fundamentals of cumulative quantum mechanics (CQM).** These quantum size effects led to the discovery of the principles of physical doping and the classification of doping into physical and chemical doping. During physical doping, the modification of the properties of the nanocomposite is carried out with the help of nanostructures of foreign material, which have a high affinity for free electrons. In this case, the fractions of foreign material do not penetrate into the crystal lattice. A dopant with a high affinity for free electrons is charged with a negative charge, while a doped nanocrystal is charged with a positive charge. Therefore, physical doping of nanocomposites leads to the generation of electric fields that act as catalysts for various reactions, contributes to the strengthening of nanocomposites by Coulomb's compression, an increase in the luminescent properties of phosphors, an increase in conductivity up to  $10^{10}$  times, and other properties, due to quantum size effects due to local violation of electrical neutrality. We used QCM to explain similar phenomena in the nano-, angstrom- and femto-world of cumulative-dissipative structures. Based on experiments and QCM, we analyzed the processes: pulsation of electric fields in quantum resonators, partial collapse of the  $\psi$ -functions, **expanded Dirac's claim about the limited of a  $\psi$ -functions and detailed the problem of the dualism in quantum mechanics – Wave-Particle.**

**KEYWORDS:** physical doping; quantum size effects; nanocomposites; cumulative quantum mechanics; de Broglie wave cumulation; unlimited cumulation of de Broglie's wave  $\psi$ -functions; cumulation-libration points; endo-electrons; fullerenes; cumulative-dissipative structures

---

## Introduction

In the leading laboratories of the world, intensive work continues to study the properties of nanostructured materials that have unique, both physical and chemical properties that are useful in practice. Along with the discovery of new materials, new technologies are being developed and attempts are being made to create mathematical models capable of describing phenomena in hollow quantum resonators—quantum dots, lines and other cumulative-dissipative 3D structures of nanometer dimensions. Such goals can be achieved by verifying and modernizing the fundamentals of the new quantum theory and supplementing it with the fundamentals of cumulative quantum mechanics (CQM), which describes real cumulative and dissipative phenomena in the nanometer regions of quantum mechanics. This modification of new wave quantum mechanics, substantiated by experiments in the nanoworld, turns out to be very useful in describing “mysterious” cumulative-dissipative phenomena in structures with sizes from  $10^{-15}$  to  $10^{26}$  m<sup>[1-6]</sup>. Our review highlights the problems that arise when describing the intrinsic energy spectra of hollow quantum nanocavities between the de Broglie hypothesis and the classical new quantum mechanics of Dirac, which limits the values of  $\psi$ -functions everywhere, are noted. It is shown how these problems and paradoxes (the discrepancy between experimental observations and incomplete theories), caused by phenomena arising from the violation of electrical neutrality in nanostructured composite materials, are solved using CQM and taking into account the regularization of unlimited  $\psi_{n-1/2}$ -functions by a normalizing geometric coefficient that takes into account symmetry of the quantum resonator.

The study of the interaction of polarizable fullerenes with electrons made it possible to discover and analytically describe all the quantum-size effects discussed in this paper. We managed to establish the characteristic dimensions on which these (quantum) effects are formed and to investigate how quantum effects manifest themselves in the mesoworld of nanocomposites and even the macroworld of quantum stars and black holes<sup>[1-6]</sup>. For this reason, the results obtained by the author on the study of quantum-size effects are successes in the physical and chemical sciences, and even in the astrophysical sciences. The models we have developed, which are effective for explaining nano-effects, have been used by us to explain angstrom and femto phenomena in cumulative-dissipative structures.

Fullerenes with trapped electrons are a class of negatively charged quantum dots or negative endoions<sup>[3-6]</sup>. The synthesis of fullerenes, which include atoms of other chemical elements inside their framework, is carried out by the same methods as the synthesis of hollow fullerenes. The first endohedral metallofullerenes La@C<sub>60</sub> and La<sub>2</sub>@C<sub>60</sub> were obtained a week after the fullerenes themselves were obtained at the Smalley's installation. In addition to metals, fullerene atoms can include atoms of helium, neon, argon, krypton, and even molecules of CO, CN, etc.

The question of the possibility of capturing free electrons into the internal cavity of fullerene was raised by P.I.Vysikaylo<sup>[3-6]</sup>. As a rule, when calculating the interaction of an electron with a fullerene molecule, the characteristic size of the trap,  $R$ , is used. Polarization effects are not taken into account. In the case of neutral atoms inside fullerenes, polarization effects are small. During the formation of the e@C<sub>60,70...</sub> endo-electron, the electrical forces of interaction between the electron and the electron shell are significant and lead to a number of quantum-size effects. These effects are explained in terms of quantum wave-particle duality. When an electron leaves a fullerene as a particle, a negatively charged electron

interacts with the electron shell and leads to its displacement (**Figure 1a**). In the case of interaction of an electron as a particle with the electron shell of a fullerene, the polarization forces reach their maximum value at a certain distance from the fullerene— $r_{ind}$ . This leads to the formation of a Coulomb mirror that focuses the electron back into the fullerene cavity (**Figure 1**). When the electron returns to the fullerene cavity, its polarization disappears and the Coulomb mirror also disappears. After the electron leaves, like a particle, from the opposite side of the fullerene, the fullerene is already polarized on this side and the Coulomb mirror returns it back into the cavity of the fullerene. Taking into account a pulsating Coulomb mirror located at a distance  $r_{ind}$ , we can then solve the problem of trapping an electron as a wave with resonant energy into a spherically symmetric resonator with a radius  $R + r_{ind}$  (**Figure 1b**).

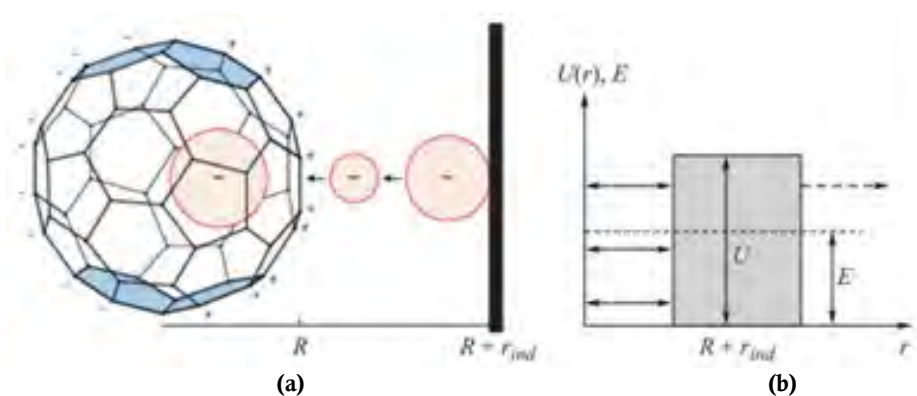


**Figure 1.** Scheme of cumulative pulsating e-capture with resonant energy electron from 0.2 to 20 eV into the cavity of a  $C_{60,70}$  molecule and resonant formation of a negative endo-ion  $e_k@C_{N=60,70,\dots}$ . Endo-ion radius (position of the reflecting "mirror"  $R_i = (R_{C_{60,C_{70},\dots}} + r_{ind})^{[2-6]}$ ;

**a**—4D (space-time) process of formation of a standing de Broglie's wave in a polarizing quantum resonator with a successive decrease in the de Broglie's wavelength of an electron incident on a fullerene molecule polarized by it<sup>[2-6]</sup>. The polarization pulsating barrier that returns the electron back to the fullerene is shown as a black rectangle on the right;

**b**—diagram of the resonance spectrum of a metastable (quasi-open) quantum particle with a polarization partially transparent mirror (of finite dimensions), which captures an electron with energy  $E > 0$  in polarization trap of characteristic size  $R + r_{ind}$ . The polarizing mirror is darkened.

As a comparison of analytical calculations<sup>[3-6]</sup> with experimental observations<sup>[7-9]</sup> of the energy spectra of such quantum dots showed, their own energy spectrum is significantly determined not only by the characteristic size of the object,  $R$ , capturing an electron, but also by the characteristic polarization size,  $r_{ind}$ , where the most effective forces acts on the electron (returning it to the trap). These forces are due to the polarization of the quantum trap for electrons. Typically, estimates use the characteristic size of the trap and do not take into account the full characteristic size of the interaction  $-R + r_{ind}$  (**Figure 1**). An electron, when captured in the fullerene region (**Figure 1**), behaves like a wave reflected from the polarization boundaries, which are located beyond the boundaries of the fullerene at a distance of  $r_{ind}$ . (In this case, the description of its behavior is reduced to the first Helmholtz's boundary value problem<sup>[10]</sup>). For  $C_{60}$  fullerene,  $R = 0.36$  nm, and  $R + r_{ind} = 0.62$  nm<sup>[3-6]</sup>. Not taking into account polarization effects during electron capture is a mistake caused by neglecting the characteristic polarization size of a nanoobject!

The main, fundamental problem of nano-chemistry and nanophysics, around which all the interests of researchers revolve, is quantum-size effects. These are intriguing questions: how the properties of individual molecules, when combined, evolve into properties of the phase; how bridges are built between the world of a single, individual molecule and the macroscopic world of matter; how the hierarchy of quantity is transformed into a hierarchy of properties, how the cumulation of various portions of energies leads to a change in the geometry of crystal lattices, a change in their properties, their hardening,

enlightenment, polarization when interacting with a charged particle or an electromagnetic field, etc.

The emergence of synergistic electric fields due to the resonant localization of electrons in traps at the boundary of a positively charged nanocrystal leads to the appearance of two types of Vysikaylo's polarization quantum-well resonance effects<sup>[3-6]</sup>. According to the Vysikaylo's polarization effect of the first type<sup>[3-6]</sup>, the capture of electrons (**Figure 1**) can occur as a result of the formation of a standing de Broglie wave in a quantum hollow resonator for these waves (Q-particles: quantum dots, wires and wells). The characteristic size of the Vysikaylo's polarization effect of the first type is determined by the characteristic size of the trap (~1 nm for C<sub>60,70</sub> and other fullerenes and nanotubes). According to the Vysikaylo's polarization effect of the second type, depending on the number of traps in the nanocomposite, the positive charge of the nanocrystallite (**Figure 2**) physically doped with traps will change. And, consequently, the average energy of electrons near the surface of nanocrystals will change on the dimensions of a positively charged crystallite or on the dimensions of a negatively charged nano-modifier. As a result, due to the polarization resonant interaction, by changing the dopant concentration (trap concentration) in the nanocomposite, it is possible to effectively control the macroparameters of bilayer (polarized due to the presence of the modifier) metamaterials with sizes from 10 nm to meso-sizes of the entire material. So, according to Vysikaylo<sup>[3-6]</sup>, we come to the discovery of a new method of doping—physical doping or the formation of bilayer (bicharged) metamaterials (**Figure 2**) and their effective application in practice, for example, when modifying the properties of phosphors<sup>[5,6]</sup>. This is how a new nano-chemistry arises—nano-electrochemistry (**Figures 1 and 2**).

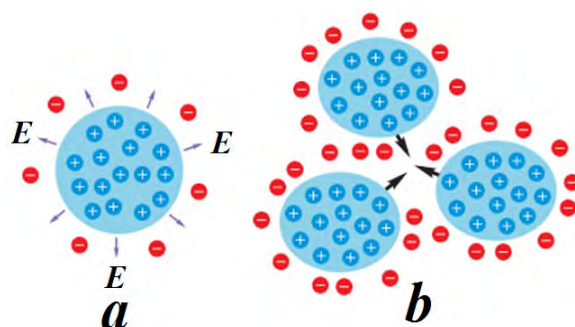


**Figure 2.** Schematic of the physical principle.

**a** - modification of the properties of composite materials by layers of space charge formed by traps for free electrons;  
**b** - diagram of the Coulomb compression of polarized complex structures. The arrows indicate the direction of the Coulomb forces compressing the nanostructured polarizable composite.

It is possible that polarization or the formation of electrical potentials can lead to local ice melting. So, due to the heating of water by electrons around positively charged microorganisms in eternal glaciers, a kind of antifreeze can form. It is possible that the accumulation of highly energetic electrons in the structures of microorganisms provides them with the opportunity to survive in such harsh conditions in the almost complete absence of energy coming from outside. In the presence of the Coulomb potential, it is possible to transfer energy from a cold body (for example, a crystal lattice) to a hot one (an electron gas with a large kinetic energy). The cumulative-dissipative structures (CDS) of living organisms are diverse and require detailed studies of electrical neutrality violation, both in living and inanimate plasma polarizable CDS.

In this work we will seek experimental confirmation of cumulative quantum mechanics (CQM), formulated by Vysikaylo [2-6] in experiments with fullerenes (hollow ideal spherically symmetric polarizable quantum dots capable of capturing free electrons with a resonant energy  $E_n \sim 0.2 \div 20 \text{ eV}$ <sup>[7-</sup>

9).

The purpose of this paper is to present 32 quantum-size effects discovered and classified by the author.

## 2. Thirty two quantum-size effects during physical doping of nanocomposites

It has long been known that a number of molecules have a high affinity for electrons, such as oxygen molecules. Because of this affinity, negative ions  $O_2^-$  and  $O_4^-$  are formed. We discussed experimental facts in detail and proved that nanometer-sized carbon structures (like fullerenes, nanotubes, nanodiamonds, and nanographenes (**Figure 1**)) have the same property of localizing free electrons. Cavities, cracks, etc. have the property to localize free electrons <sup>[2-6]</sup>. The use of physical doping of nanocomposites significantly changes their properties in the mesoworld (**Figure 2**)<sup>[2-6]</sup>.

Violation of electrical neutrality (polarization) at the nanolevel leads to thirty two polarization quantum-size effects discovered by Vysikaylo<sup>[2-6]</sup> and this work. Let's list these effects:

**Effect 1**—Coulomb hardening (compression, focusing, reduction, cumulation) of positively charged nanocrystals by nanolayers of negatively charged electron traps (**Figure 2b**)<sup>[2-6]</sup>. This quantum size effect was experimentally studied on the example of physical doping with carbon nanostructures of such materials as semiconductors (thermoelectrics), copper, aluminum and transition metal carbides<sup>[4-6]</sup>. According to experimental observations, copper and aluminum were physically hardened by doping with fullerenes up to 10 GPa<sup>[4-6]</sup>, and copper films were strengthened by graphite nanostructures up to 4 GPa<sup>[4-6]</sup>. Hardening of transition metal carbides by physical alloying of films with carbon nanostructures by magnetron sputtering was registered up to 31 GPa. In this case, strengthening by physical alloying of nanocomposites with a nanocrystal size of ~20 nm up to 100 GPa is considered theoretically possible<sup>[4-6]</sup>. However, maintaining a size of 20 nm for all nanocrystals in a nanocomposite is a complex technological problem.

**Effect 2**—according to Newton's third law, the cohesive forces and the forces of resistance to compression in crystalline materials are equal to each other<sup>[5]</sup>. Hardening of the material, including physical alloying (**Figure 2b**), corresponds to the same increase in the microhardness of the nanocomposite. Nanocomposite materials can be strengthened by creating nanosized graphene shells covering composite nanocrystals.

**Effect 3**—generation of electric fields (up to  $10^{11}$  V/m) and potentials that "heat" electrons in the area of the nanocrystal surface (**Figure 2a**)<sup>[4-6]</sup>. During physical doping, the properties of the surface of volumetrically charged nanocrystals also change due to the polarization of charges at the nanolevel (sizes of physically alloying nanoadditives), see **Figure 2**, for example, due to an increase in the average energy of free electrons on the surface of nanocrystals. Experiments have shown that this leads to an increase in the luminescent characteristics of the phosphor by up to 50%<sup>[4-6]</sup>.

**Effect 4**—generation of electric fields (up to  $10^{11}$  V/m) and potentials that "heat" electrons in the area of the nanocrystal surface (**Figure 2a**)<sup>[4-6]</sup> leads to the appearance of catalytic properties in physically doped nanoparticles. This is due to a local increase in the electrons kinetic energy (decreasing their de Broglie wavelength) in the area of the surface of a positively charged nanocrystal and the possibility of them penetrating through Coulomb's barriers.

**Effect 5**—the electric field strength on the surface of a nanocrystal depends on the concentration of



nanotraps on the surface of a physically doped material<sup>[4-6]</sup>. This effect leads to a change in the energy of electrons on the surface of a physically doped nanocomposite with a change in the concentration of traps and, as a consequence, leads to a change in the number of electrons trapped in an electron quantum resonator (nanotrap). If only the resonant spectrum of localized electrons is possible in a quantum resonator, as in fullerene C<sub>60</sub><sup>[4-6]</sup>, then the concentration-polarization-quantum-size Vysikaylo's effect of the second type will be observed in the corresponding range of parameters (**Figure 3**). In this case, the profiles in **Figure 3a** shift with a change in the characteristic radius of the nanocrystallite, forming a quantum size pair with a relative concentration of traps). With this quantum size effect, with a change in the relative concentration of the physically alloying additive, the parameters of the nanostructured composite in the mesoworld change<sup>[4-6]</sup>. Using this quantum size effect, the properties of thermoelectrics can be modified by changing the concentration of nanocarbon particles in the nanocomposite<sup>[4-6,11]</sup>. In experiments<sup>[11]</sup>, it was possible to increase the efficiency of a thermoelectric by 30% due to physical doping with fullerenes.

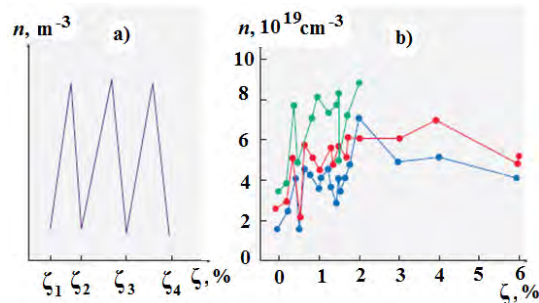


**Figure 3.** Concentration-quantum-dimensional Vysikaylo's effect: **(a)** the characteristic dependence of the nanocomposite parameter, for example, the concentration  $n$  of ions or electrons, on the volume content of C<sub>60</sub> in the composite; **(b)** experimental measurements of resonance profiles of electron density with a change in the relative concentration of traps during physical doping of semiconductor nanocrystals (thermoelectrics) with C<sub>60</sub> fullerenes at various temperatures (77–295 K); The characteristic size of a nanocrystallite after annealing is  $D \approx 17 \text{ nm}^{[11]}$ .

**Effect 6**—generation of electric fields (up to  $10^{11} \text{ V/m}$ ) and potentials “heating” (decreasing their de Broglie wavelength) electrons locally in the area of the nanocrystal surface (**Figure 2a**)<sup>[4-6]</sup> can lead not only to dynamic hardening of physically doped nanocrystals, but weak modification of their crystal lattice for nanocomposites. This effect manifests itself more significantly in quantum stars, where the strengthening membrane is a layer of electrons or negative mesons rather than fullerenes<sup>[1,5]</sup>, (**Figure 2a**);

**Effect 7**—in nanocomposites, the pair “eigen-function  $\psi_n$ —eigen-energy  $E_n$ , describing the quantum state with the principal quantum number  $n$ , in the nanoworld, in the mesoworld of nanocomposites physically doped with traps, is replaced by two parameters of the nanoworld: the diameter of the nanocrystal  $D$  and the relative concentration of the modifier (traps, for example, C<sub>60</sub>)— $\zeta_n$  (**Figure 3**)<sup>[4-6]</sup>.

**Effect 8**—self-focusing of the charge and electric field in nanostructures due to polarization forces arising from the interaction of nanostructures with electrons in nanostructures with high electron affinity. For example, according to experimental data<sup>[12]</sup>, fullerene can accumulate up to six electrons per one C<sub>60</sub>, which corresponds to electric fields around the fullerene of  $\sim 10^{10} \text{ V/m}$ . This phenomenon is a polarization cumulation (localization) of free electrons in a trap, i.e., quantum resonator.

**Effect 9**—cumulation (localization) of the energy of free electrons in a trap—a quantum resonator. For example, according to experiments<sup>[12]</sup>, fullerene can accumulate up to six electrons per C<sub>60</sub> with a resonant kinetic energy from 0.24 to 12 eV. This can lead to the accumulation of the energy of the electron gas up to 30 eV in one fullerene.

**Effect 10**—the presence of polarization forces of cumulation (focusing) of charged particles in quantum resonators (traps). To describe the capture of an electron in  $C_{60,70\dots}$  (with an ideal spherical shape), the author used a mathematical model developed by Gamow (to describe the penetration of an  $\alpha$ -particle through the potential barrier of an atom)<sup>[2-6]</sup>. The modified Gamow's model made it possible to analytically calculate the resonant energy levels of trapped electrons for all spherical quantum resonators ( $C_{60}$ ,  $C_{70}$  and higher fullerenes)<sup>[2-6]</sup>. From a comparison with experiments, we managed to determine the effective polarization sizes for various fullerenes (rind for  $C_{60}$ —0.26 nm and for  $C_{70}$ —0.28 nm<sup>[2-6]</sup>) at which a polarization potential barrier with a height about 18 eV, returning the electron back to the fullerene cavity<sup>[5]</sup> (**Figure 1**).

**Effect 11**—resistance to swelling during physical doping of materials with electron traps. This is a consequence of quantum size effects 8 and 9, i.e., the possibility of capturing free energetic electrons in a high-strength nanoscale trap.

When materials are subjected to: energy loading, for example, when: irradiated with neutrons, electromagnetic radiation or subjected to: bending, friction or other functional energy loads, there is an accumulation of energy coming from outside into the material. In a material, energy is accumulated mainly in a localized electron gas. Let us detail this process of energy accumulation in a functioning material. The electrons in the material are in the Coulomb potential wells of atomic nuclei. And with an increase in the total energy of an electron in the Coulomb well, its kinetic energy decreases. According to the foundations of quantum mechanics, the de Broglie wavelength of such an electron increases; consequently, an atom with such an electron in the “orbit” swells, and if there are many of them, then the entire functioning material swells significantly. According to Newton's third law, an excited atom is opposed by a medium. Consequently, the excitations will be displaced to the surface and self-focus on the internal inhomogeneities of the functioning material. As the number of excited atoms in the loaded materials increases, a noticeable local swelling is observed, as well as the growth of cracks and a change in other physical and chemical properties, leading to a deterioration in the functional properties of the material and even to its destruction. Expansion and self-focusing processes (cumulation and localization) during swelling promote the formation and growth of cracks and the localization of free electrons in cracks or cavities. Further filling of cracks with free electrons, as the most mobile and bulk gas, is determined by the movement of free electrons from the material into the crack and the reflection of electrons by the crack boundaries back into the crack. This happens in the same way as in the case of polarization capture of an electron by fullerene (**Figure 1**). In a crack with a large number of electrons, the electron energy distribution function (EDF) is formed. This is due to electron-electron collisions. Since the crack geometry, as a rule, has a conical shape, high-energy electrons are displaced to the crack tip region, where they transfer its kinetic energy into the potential energy of crack growth. An increase in the pressure of the electron gas localized in the crack and the geometry of energy cumulation at the crack tip leads to catastrophic crack growth and destruction of the material, which very quickly dissipates the energy accumulated in the working material into cracks. An increase in the number of excited electrons in the region of a cavity or crack leads first to its slow and then to catastrophic explosive growth, since the material gets tired and excess kinetic energy of electrons accumulates in it, which transforms into potential energy concentrated in cracks. The introduction of the durable nanometer traps for free electrons  $C_{60}$  (with a resonant energy spectrum for inner electrons of 0.24–12 eV) into physically doped nanocomposites in small amounts, which do not significantly change the useful properties of nanocomposite materials, makes it possible, under a number of conditions, to reduce the number of free electrons and thereby weaken the catastrophic swelling and crack growth in functional materials

subjected to energy loading. These hollow spherical heavy-duty resonators— $C_{60}$  are capable of concentrating up to six electrons<sup>[12]</sup> with a total energy of up to 30 eV<sup>[5,6]</sup>. In this case, the strength of the fullerene framework corresponds to the strength of graphene and exceeds the strength of diamond. In this regard, such a spherically symmetric trap, unlike a cavity or a crack, does not increase in volume and does not swell, which significantly increases the catastrophic fracture threshold of a nanocomposite physically doped with high-strength traps for free electrons. Such physical alloying increases the service life of the nanocomposite, its reliability and duration of operation under conditions of intensive operation.

**Effect 12**—levitation (floating, repulsion) of positively charged nanostructures of a physically alloyed material one above the other (**Figure 2b**). This effect counteracts the processes of recrystallization in nanocomposites, which significantly increases the characteristic time of their operation<sup>[4-6]</sup>. Let us note that the violation of electrical neutrality of matter at the level of  $10^{-18}$  (for one proton uncompensated by a negative charge,  $10^{18}$  compensated) stops the gravitational collapse of even black holes<sup>[1,5]</sup>.

**Effect 13**—Coulomb's melting of nanofullerite (fullerene nanocrystals), which occurs when  $k$  electrons are captured by fullerene molecules in fullerite. In a fullerite crystal,  $C_{60}$  molecules are bound together by weak van der Waals forces. The binding energy of a single fullerene molecule in a fullerite nanocrystal does not exceed 1.6 eV<sup>[13]</sup>. In this case, the potential energy of the Coulomb's interaction of two negative ions in fullerite with  $k$  electrons is of the order  $1.4 \times k^2$  [eV] (the average distance between fullerenes in fullerite is  $D \approx 1$  nm). Thus, the capture of several electrons from a nanocrystal physically doped with fullerenes leads to Coulomb's sputtering of fullerite nanostructures and a monolayer coating of a positively doped nanocrystal with negatively charged fullerenes (**Figure 2b**)<sup>[4-6]</sup>. One  $C_{60}$  fullerene molecule is capable of capturing up to six electrons<sup>[12]</sup>. Note that, in principle, neither nanotubes due to their entanglement or interweaving, nor nanographenes due to their strength, have such a property to decompose into strictly nanosized structures. In experiments, it is this property of fullerites that made it possible to create materials by physically doping thermoelectrics<sup>[11]</sup>, copper<sup>[4-6]</sup>, and aluminum<sup>[4-6]</sup> with  $C_{60}$  fullerenes, which have unique functional and strength properties. Our theory predicts the possibility of increasing the microhardness of a physically doped nanocomposite with fullerenes up to 100 GPa<sup>[4-6]</sup>.

**Effect 14**—cumulation of electron flows at points (lines and planes) of libration between positively charged nanostructures (**Figure 4b**—cumulation-libration point— $L_1$ ). These effects have been studied in gas-discharge plasma<sup>[14]</sup> and are still insufficiently detailed in nanocomposites. This cumulative quantum size effect, caused by the capture of free electrons with resonant energy in a quantum resonator and the formation of positively charged nanocrystals of a doped material, can be used to control local parameters: conductivity, thermal conductivity, and other properties of nanocomposites.

**Effect 15**—when a charged particle interacts with a system containing an electron gas or a Fermi liquid, due to the high mobility of electrons in any systems, it leads to the formation of polarization barriers that cumulate these particles to the center of a hollow polarizing system (**Figure 1**). This approach now allows us to detail the essence of the polarization barrier introduced by Gammov for the  $\alpha$ -decay of atomic nuclei. Such dynamic barriers arise for short times when a charged particle tends to leave a polarizing pulsating system<sup>[2-6]</sup>. Therefore, such dynamic barriers cannot be modeled using DFT methods<sup>[15]</sup> (density functional theory). To calculate the resonant energy spectrum, we replaced such a pulsating partially transparent barrier with a stationary barrier surrounding the fullerene (**Figure 1a**).

**Effect 16** is the counteraction of electrons in the trap to external action on the trap and on the entire nanocomposite material (**Figure 1a**). In this case, electrons having de Broglie wavelengths larger than the dimensions of the polarizing trap counteract the external action, protecting the physically doped material



from destruction;  $R$  is the radius of the trap;  $r_{\text{ind}}$  is the characteristic induction size by which the electron leaves the trap (**Figure 1b**). In experiments, this effect was observed when metal products were coated with graphene sheets. This effect was used to explain the properties of a white dwarf in astrophysics by Frenkel and Fowler. It turns out that any electrons localized in a polarizing Coulomb well in any quantum resonators with sizes from  $10^{-15}$  (in this case, negative mesons play the role of electrons) to  $10^{26}$  m have dual properties—to focus the structure and counteract its compression (**Figure 4**)<sup>[5]</sup>.

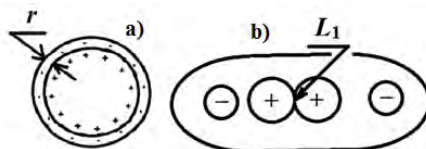


**Figure 4.** Scheme of quantum self-polarization of molecular structures on nano- and angstrom sizes<sup>[5,6]</sup>: **(a)** polarized drop with e-membrane; **(b)** an example of a covalent bond of two atoms that share external electrons, for example, in a molecule or a singly ionized hydrogen ion, if one external electron is removed.  $L_1$  is the cumulation point for electrons<sup>[5,6]</sup> between positively charged elements of the structure.

**Effect 17** is a significant change in the conductivity of materials physically doped with nanostructures from allotropic forms of carbon. For example, the use of nanotubes can lead to quantum ballistic conduction effects in negative ions from nanotubes that trap electrons. In experiments, the method of physical doping with nanotubes makes it possible to change the conductivity of the initial siloxane by 10 orders of magnitude<sup>[4]</sup>. **If for the polarization length  $C_{60}$  of fullerenes, which, according to quantum mechanics, an electron localized by the polarization potential could move, is of the order of  $r_{\text{ind}} = 0.26$  nm, and for  $C_{70}$ — $r_{\text{ind}} = 0.28$  nm (Figure 1), then for a carbon nanotube the polarization length  $r_{\text{ind}}$  is determined by its length  $L$ <sup>[2-6]</sup>.** This leads to a significant decrease the lower eigenlevel (resonant) energy of the quantum resonator for electrons and its tendency to a continuous spectrum with increasing length  $L$ .

**Effect 18**—increased emission during physical doping with nanotubes. According to effect 8, much more free electrons with resonant energy can be localized around and in the nanotube, which can significantly increase the efficiency of nanotubes in emission phenomena compared to fullerenes. A decrease in the lower energy level of the nanotube leads to an increase in the frequency of ejection of electrons previously captured by the nanotube. **The analytical calculations for fullerenes<sup>[2-6]</sup> were confirmed in a number of experiments<sup>[4,11]</sup>, such calculations for nanotubes give ambiguous results. These ambivalent (dual) conclusions for polarized carbon nanotubes should be verified in experiments with nanotubes having a given length  $L = \text{const}$ <sup>[2-6]</sup>.**

**Effect 19**—quantum size polarization effects should be taken into account in the case of many-particle interaction of atoms and molecules in dense media<sup>[5,6]</sup>. Such an allowance leads to an increase in the time of capture of several particles into a polarization trap (in the region of the polarization barrier common to several particles) and to an increase in the effective polarization cross section to a value  $\sim \pi(R + r_{\text{ind}})^2$ . Here  $R$  is the radius of the cross section without taking into account polarization, and  $r_{\text{ind}}$ —the polarization length (**Figure 1**). This leads to an increase in the effective calculated cross sections for three-particle interactions of atoms, molecules, and more complex atomic structures. Accounting for a significant increase in the effective cross sections of reactions at elevated pressures leads to the solution of a number of paradoxes (inconsistencies between experimental results and theoretical concepts)<sup>[5]</sup>.

**Effect 20**—comparison of the quantum-size effects of Vysikaylo and Casimir. This effect was discovered by Theo Overbeek. He found that the theory used to explain the van der Waals forces could

not adequately explain the data of his experiments, which showed the existence of a more significant coupling between long molecules. Casimir suggested<sup>[16]</sup> that the interaction between two neutral approaching molecules can be described if vacuum fluctuations and the generation of electromagnetic radiation—light (**Figure 5a**) are taken into account.

Between the mirrors, it is impossible to generate electromagnetic radiation with wavelengths greater than  $d$ . But it is possible outside of these mirrors. The pressure of these electromagnetic waves on the mirrors from the outside leads to the Casimir's effect. The attraction of metal plates in the Vysikaylo's effect is explained similarly. "+"—ions of the crystal lattice, "—"—free degenerate electrons with large de Broglie wavelengths, quantum-mechanically squeezed out of the space between the polished plates. The electrons squeezed out of the gap with their pressure, due to their kinetic energy, compress the plates with pressure  $P = F/S$ <sup>[17,18]</sup> (**Figure 5b**). For relativistic electrons, the dependence of pressure— $P$  (force— $F$ ) in the Vysikaylo's and Casimir's effects is  $\sim d^{-4}$ , and for the non-relativistic case the Vysikaylo's effect  $\sim d^{-5}$  (for Casimir's effect  $\sim d^{-4}$ )<sup>[4,5]</sup>.

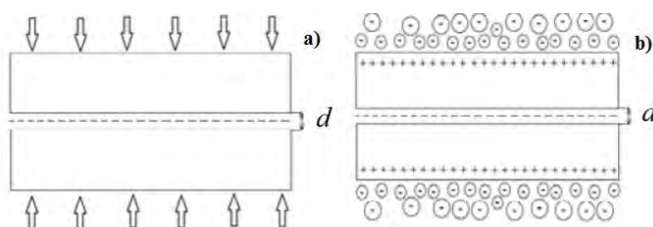


**Figure 5.** Effect scheme: **(a)** Casimir's effect. The arrows show the forces compressing the plates; **(b)** nano- and femto-dimensional quantum Vysikaylo's effect<sup>[4,5]</sup>.

**Effect 21**—the valency of an atom in a molecule is determined by the number of possible libration points— $L_1$  for electrons around an atom in a molecule (**Figure 4b**)<sup>[14]</sup>.

**Effect 22**—Vysikaylo-de Broglie-Fraunhofer's interference of de Broglie waves of electrons in hollow quantum resonators leads to unlimited cumulation of  $\psi$ -functions of de Broglie electron waves in hollow spherical and cylindrical quantum resonators (**Figure 6**)<sup>[2-6]</sup>.

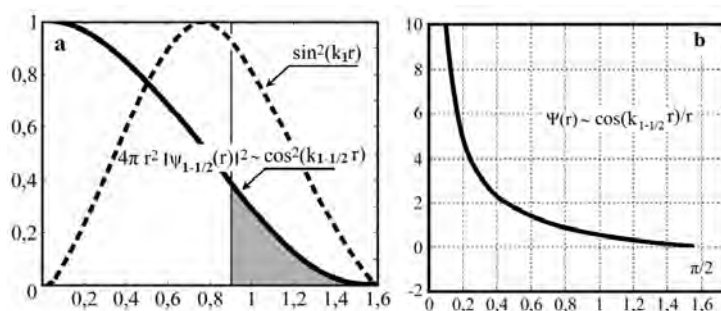


**Figure 6.** Profiles<sup>[4]</sup>: **(a)** relative probability  $4\pi r^2 |\psi_n(r)|^2 dr$  to find an electron in the region of a hollow spherically symmetric molecule, taking into account the geometric normalization coefficient. For an electron with energy,  $E_{1/2}$  (Vysikaylo-de Broglie-Fraunhofer's interference of de Broglie waves of electrons in hollow quantum resonators) is denoted by a solid line, and for an energy resonance,  $E_1$  (Bohr-de Broglie-Fresnel's interference of de Broglie waves of electrons in) is indicated by a dashed line. A straight vertical line separates the internal and external regions of a hollow polarizable spherically symmetric molecule. The relative probability of finding an electron at  $1/2$ -resonance (cos-wave) outside the shell of a hollow molecule is shaded (calculations were made for  $C_{60}$ ); **(b)**  $\psi_{1/2}$ -functions at  $1/2$ -resonance (cos-wave with  $E_{1/2}$ ).

**Effect 23**—eigen-energy spectra of hollow quantum resonators have a new class of solutions with eigen-energy spectrum  $E_{n-1/2} \sim (n-1/2)^{\pm 2}$  for potential wells "−", and for structures with potential barriers "+". This is how the degeneration discovered by Vysikaylo<sup>[2-6]</sup> appeared.

**Effect 24**—in hollow quantum resonators, transitions with the corresponding resonance spectrum are possible not only between sin-waves, but also all transitions between cos- and sin-states of de Broglie waves<sup>[2-6]</sup>. Thus, we discovered several times more allowed spectra in hollow quantum resonators than in ordinary atoms, where there are no stationary cos-resonances. This is the degeneracy of the ground quantum level  $n$  in sin- and cos-waves in hollow quantum resonators<sup>[2-6]</sup>. The author was the first to discover the splitting of the ground quantum level  $n$  into sin- and cos-waves in hollow quantum resonators (Figure 7)<sup>[3-6]</sup>. This Vysikaylo's splitting was experimentally discovered earlier in experiments<sup>[7-9]</sup>, but was not explained by the experimenters.

**Effect 25**—self-energy spectra of quantum resonators do not depend on the type of their symmetry<sup>[2-6]</sup>. As shown by us, in accordance with the de Broglie's hypothesis, in QCM the eigen-spectra of quantum hollow resonators do not differ from each other for all three types of symmetry: spherical, cylindrical, and planar, and they are determined only by the characteristic size of the resonator<sup>[2-6]</sup>.

**Effect 26**—in the theoretical description of cumulation phenomena in spherically and cylindrically symmetric resonators, it is necessary to take into account the normalization geometric coefficients that regularize the probability of finding a particle in a layer<sup>[2-6]</sup>. This is often forgotten in quantum mechanics textbooks. Part of the solutions of the Schrödinger's equations (the first Helmholtz boundary value problem) for this reason are thrown out without any reason for hollow quantum resonators.

**Effect 27**—in quantum hollow resonators with any type of symmetry, de Broglie's standing waves of electrons with half a wavelength are possible<sup>[2-6]</sup>. **This was proven by comparing analytically calculated calculations of the intrinsic energy spectra of C<sub>60</sub> quantum resonators with experimentally obtained profiles of resonance cross sections<sup>[7-9]</sup> using the example of electron capture C<sub>60</sub>, C<sub>70</sub> (Figure 7)<sup>[2-6]</sup>.**

**Effect 28**—we have proved that when applying the de Broglie's hypothesis from the femtodimensional to the mesoworld and the world of galaxies, it is necessary to carry out not a partial, but a complete transfer of mathematical models from areas well studied in the field of natural sciences, studied insufficiently<sup>[2-6]</sup>. It is necessary to investigate the whole range of similar phenomena, and not be limited only to particular solutions. So, in wave physics such phenomena as cavitation and sonoluminescence in acoustic resonators have long been known. These phenomena are due to the cumulation of wave energy towards the center of the acoustic resonator. In this paper, we point out the phenomena of unlimited cumulation of  $\psi_{n-1/2}$ -functions of quantum particles in hollow quantum resonators with spherical and cylindrical symmetries (Figure 6b).

**Effect 29**—during polarization resonant capture of an incident plane de Broglie wave of an electron into a hollow spherically symmetric quantum polarizable resonator with a high electron affinity, the de Broglie plane wave  $\psi \sim \exp(ik_{n,n-1/2}x)$  is modified into a spherically symmetric wave with  $\psi \sim \sin(k_n r)/r$  or  $\psi \sim \cos(k_{n-1/2} r)/r$ . The reverse transition occurs in the case of penetration of a spherically symmetric de Broglie wave through a potential polarization barrier (Figure 1). This effect is proved by agreement of experimental observations of the resonance spectra of e-capture by fullerenes (Figure 7) with our theoretical studies<sup>[6]</sup>.

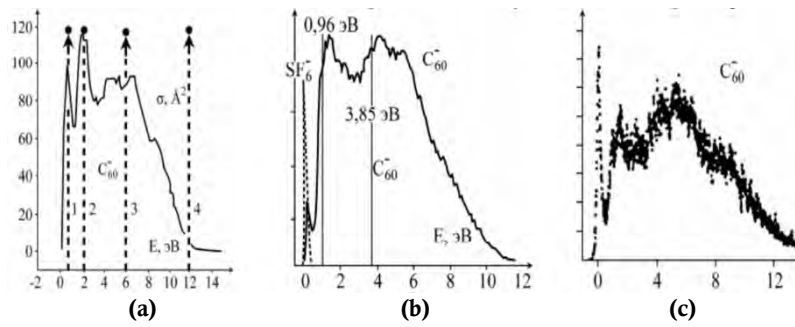


**Figure 7.** Comparison of theoretical calculations (3)–(4) and experimentally measured e-capture cross sections [ $\text{\AA}^2$ ] in  $C_{60}$  depending on the electron energy: **(a)** for  $C_{60}^{[8]}$ . Straight bold vertical lines mark the eigenenergies for cos-waves in  $C_{60}$  (with principal quantum numbers  $n = 1\frac{1}{2}, 2\frac{1}{2}, 3\frac{1}{2}, 4\frac{1}{2}$ ), calculated analytically (3) taking into account the effect of  $C_{60}$  polarization forces on the stabilization of the fullerene endo-ion (**Figure 1a**); **(b)** relative electron attachment cross sections to  $SF_6$  and  $C_{60}$  for the  $C_{60}$  flow ( $T = 673\text{ K}$ )<sup>[9]</sup>. Straight vertical lines mark the eigenenergies for sin-waves in  $C_{60}$  (4) with principal numbers  $n = 1, 2$ , calculated analytically, taking into account the polarization of  $C_{60}$  on stabilization of the fullerene endoion; **(c)** experimental curves of the effective yield of resonant e-capture by  $C_{60}$ <sup>[7]</sup>.

Let's consider the problem in more detail from the point of view of quantum wave-particle dualism. As noted earlier, an electron incident on a fullerene, as a negatively charged particle, polarizes the fullerene molecule (**Figure 1a**) and, penetrating the fullerene, is reflected back to its center by a polarizing pulsating mirror (**Figure 1b**). This mirror is formed at a distance  $R + r_{ind}$  from the center of the fullerene (**Figure 1**).

To analytically determine the resonant energy spectrum of electrons captured by  $C_{60}$  fullerene, we will use the *stationary Schrödinger equation* to describe the de Broglie wave function of the electron:

$$\Delta\psi_n + (2m/\hbar^2)(E_n - U)\psi_n(r) \quad (1)$$

With the boundary conditions: when  $r < R + r_{ind}$ , then  $U = 0$ . At  $r > R + r_{ind}$ , then  $U = \infty$ —polarizing mirror (**Figure 1**). Here we have moved from an electron as a particle to an electron as a spherically symmetric wave in a quantum resonator with a characteristic radius  $R + r_{ind}$  (**Figures 1 and 6**).

Solutions that satisfy Equation (1), with the specified boundary conditions, for all types of symmetry are known in the case of the first boundary value problem<sup>[10]</sup>—these are functions with angular momentum relative to the center of the resonator  $l = 0$ :

$$\psi_n = (A_n \sin(k_n r) + B_n \cos(k_n r))/r^\gamma \quad (2)$$

and a number of known solutions in the form of a product of Bessel functions and associated Legendre functions with  $l \neq 0$ . Below we will omit the analysis of solutions with Bessel and Legendre functions with  $l \neq 0$  and limit ourselves only to the analysis of the solutions in the Equation (2). Here  $k_n^2 = (2m/\hbar^2)(R + r_{ind})^2 E_n > 0$ ,  $\gamma = 1$  for the case of spherical and  $\gamma = 0.5$  for the case of cylindrical symmetry, for the case of plane symmetry  $\gamma = 0$ .

According to Equations (1) and (2) and **Figure 1**, both in planar resonators and in any spherically or cylindrically symmetric resonators, resonant standing sin-waves with  $k_n(R + r_{ind}) = n\pi$ ,  $n = 1, 2, 3, \dots$  and cos-waves with  $k_n(R + r_{ind}) = (n - \frac{1}{2})\pi$ , if we consider solutions relative to the center of the resonator (**Figures 1 and 6a**). Therefore, for sin-waves:

$$E_{n\sin} = (\hbar^2/2m)\pi^2 n^2 / (R + r_{ind})^2, \quad n = 1, 2, 3, \dots$$

for cos-waves:

$$E_{n\cos} = (\hbar^2/2m)\pi^2 (n - \frac{1}{2})^2 / (R + r_{ind})^2, \quad n = 1, 2, 3, \dots$$

Analytical calculations of the resonance energies of electrons for  $C_{60}$ ,  $C_{70}$  and higher fullerenes

undertaken according to the model of quantum resonances, proposed by the author, qualitatively and quantitatively agree well with the experiments<sup>[7-9]</sup> (**Figure 7**), if cos-waves are considered. Thus, **the analytically calculated resonances for cos-waves (of the principal tone) in C<sub>60</sub>**<sup>[3]</sup>:

$$E_{n-\frac{1}{2}} = 0.24; 2.2; 6.0; 11.8 \text{ [eV]}, n = 1, 2, 3, 4, \dots \quad (3)$$

and for the sin-waves (overtones):

$$E_n = 0.96; 3.85; 8.66 \text{ [eV]}, n = 1, 2, 3. \quad (4)$$

A comparison of analytical calculations in the framework of cumulative quantum mechanics<sup>[3-6]</sup> with experimental observations of the resonant energy spectrum<sup>[7-9]</sup> (**Figure 7**) leads to conclusions:

1) Dirac's requirement that the  $\psi$ -functions of de Broglie waves be bounded everywhere is excessive. In cumulative quantum mechanics, we replace this requirement with the limited probability of finding a particle in the effective volume of a hollow quantum resonator<sup>[3-6]</sup>. To justify the lower energy level with a resonance energy of 0.24 eV observed in all experiments<sup>[7-9]</sup>, it is necessary to involve cumulative quantum mechanics<sup>[3-6]</sup>, which allows the existence of cos waves with unlimited cumulation of the  $\psi$ -function to the center of a hollow quantum resonator. Within the framework of new quantum mechanics with the Dirac requirement, it is impossible to reconcile the characteristic dimensions of  $R + r_{\text{ind}}$ —C<sub>60</sub> fullerene ( $R = 0.36$  nm and polarization barrier— $r_{\text{ind}} = 0.26$  nm). Only a cos-wave **(3)** (**Figure 6b**) with unlimited cumulation of the  $\psi$  function towards the center of the quantum resonator—C<sub>60</sub> can have such low energy. And, these waves are prohibited by Dirac's requirement that the  $\psi$ -functions are bounded everywhere. The lower level for a sin wave with a  $\psi$ -function limited everywhere has an energy of 0.96 eV **(4)**. Note that the analytically calculated energy spectrum **(3)** and the effective cross section for electron capture by fullerene  $\sigma = \pi(R + r_{\text{ind}})^2 = \pi(6.2 \text{ [\AA]})^2 = 120 \text{ \AA}^2$ , with an energy of 0.24 eV, almost exactly coincide with the experimentally measured energy spectra and a maximum cross section of  $120 \text{ \AA}^2$ , measured experimentally<sup>[8]</sup> (**Figure 7a**). The above facts experimentally and theoretically prove the validity of the application of cumulative quantum mechanics, which takes into account cos waves **and their energy spectrum (3)**<sup>[3-6]</sup>. In the general case, it is necessary to take into account the cos-waves  $\psi$ -functions of de Broglie waves that cumulate indefinitely towards the center of a hollow spherically (**Figure 6b**) or cylindrically symmetric quantum resonator.

2) When describing experiments with the polarization of quantum resonators, it is necessary to simultaneously take into account the quantum-mechanical dualism—wave-particle. It is generally believed (**Wikipedia**) that “Wave-particle duality is the concept in quantum mechanics that quantum entities exhibit particle or wave properties according to the experimental circumstances”. In this paper we draw attention to the fallacy of this opinion. Polarization potentials, which play the role of mirrors that cumulate charged particles into the cavity of the quantum resonator, are determined by the distance of the charged particle from the center of the quantum resonator. ***If we consider the electron as a symmetrical wave shell, then, due to the symmetry of the problem, a polarization mirror does not arise!*** A polarizing mirror that returns an electron to the fullerene cavity theoretically appears only when taking into account that the electron is a charged particle (corpuscle) constantly, flying past the center of the fullerene, polarizes the fullerene asymmetrically (**Figure 1a**).

3) We have proven (based on the theory of cumulative quantum mechanics<sup>[3-6]</sup> and experiments<sup>[7-9]</sup>) that particles behave like corpuscles at times on the order of the time of flight of a quantum resonator, which is accompanied by the formation of polarization barriers and their significant role in the characteristic dimensions of the quantum resonator— $R + r_{\text{ind}}$  (**Figure 1a**). And only a statistical description of the time-extended process of constant pulsation of a particle with resonant energy in a



quantum resonator with established effective boundaries is possible *in the form of spherically symmetric waves* in a spherically symmetric quantum resonator (**Figure 1b**). The quality factor of a quantum resonator with a trapped electron with a resonant energy for  $C_{60} \sim 10^{15}$ [8].

4) our analysis of experiments on the capture of electrons with resonant energy<sup>[7-9]</sup> and comparison with our analytical calculations (3)-(4)<sup>[3-6]</sup> within the framework of our cumulative quantum mechanics allows us to assert that the particle  $\psi$ -function appears only when boundary conditions are set for the Schrödinger equation (1). This means that a particle always remains a particle, and *the wave properties of the particle correspond to its statistical behavior in a quantum resonator and are determined by the boundary conditions*. This means that in the case of two slits, the interference pattern appears only as a statistical result. The representation of a free particle as a moving plane de Broglie wave is wrong! The particle itself does not turn into a shell, a plane wave, etc. *The particle statistically behaves like a wave in a particular resonator, and this behavior creates the effect of its transformation into a wave or shell*. When the characteristic dimensions of quantum resonators change, the  $\psi$ -function of a quantum particle captured in the resonator can be modified, for example, when an electron collapses into a proton in an atomic nucleus, etc. In this regard, wave cumulative quantum mechanics is an analogy of the wave mechanics of liquids and has a number of analogues.

**Effect 30**—in quantum resonators (complex quantum particles) are observed to be reflected from polarization boundaries (Coulomb's barriers) (**Figure 1**). Reflection from atomic nuclei and protons of de Broglie's waves of weakly energetic electrons is proved by the absence of spectra of cos-waves in the hydrogen atom and hydrogen-like atoms. These provisions are proved by comparing analytical calculations of resonant energy spectra with numerous experiments, both with fullerenes (**Figure 7**) and with hydrogen-like atoms, the spectra of which are described by the Schrödinger's equation<sup>[5,19]</sup>.

**Effect 31**—when a free electron (de Broglie plane wave) is captured by hollow resonators, for example, fullerenes or nanotubes, a transformation (partial collapse) of the electron  $\psi$ -function occurs. When a previously free electron is captured, its  $\psi$ -function transforms from a plane wave into a spherical or cylindrical  $\psi$ -function. As a result, in a hollow quantum resonator with a trapped electron, a complex cumulative-dissipative structure pulsating in time is formed with vibrational states formed due to the presence in the system of a self-consistent electric field, which is constantly present in all quantum systems with charged particles and their energy resonance spectra. All the electrons in these systems pulsate as de Broglie waves inside this electron trap. Quantum traps with trapped wave particles can emit electromagnetic waves or release quantum particles after a certain time into the environment surrounding the trap. The characteristic times of partial collapse  $\psi$ —a function of a quantum particle in a polarizable quantum resonator can be estimated from  $(R + r_{\text{ind}})/v$ . Here  $R + r_{\text{ind}}$  is the distance to the polarization barrier,  $v$  is the velocity of the particle incident on the resonator. For electrons with an energy of about 1 eV incident on a fullerene with a characteristic size of  $R + r_{\text{ind}} \approx 0.62$  nm, the pulsation (partial collapse) time is about  $10^{-15}$  s. When an electron collapses into a proton (with e-capture of an electron by an atomic nucleus), the collapse time is about  $10^{-23}$  s. Here we applied the principles of quantum dualism for these estimates, see Effect 29.

**Effect 32**—The analysis of numerous experimental works on the study of collapse or e-capture allows us to state the following<sup>[5]</sup>:

- 1) The phenomena of cumulation and dissipation are not limited by atomism, as stated by E. I. Zababakhin<sup>[20]</sup>.
- 2) We were the first to propose a general mechanism for the collapse (cumulation and transformation)

of plane de Broglie waves of electrons into spherical waves in fullerenes, atoms and into protons during the e-capture into atomic nuclei<sup>[5]</sup>. These three types of spherical e-cumulation are accompanied by corresponding collapses of the electric field of the polarizing fullerene and electron at sizes  $10^{-9}$  m; in the atomic region at sizes  $\sim 10^{-10}$  m and similarly in the proton region in the atomic nucleus with the transformation of this proton into a neutron at sizes  $\sim 10^{-15}$  m.

- 3) The probability of finding an electron as a stationary de Broglie wave in the center of hydrogen-like atoms is zero. This suggests that stationary de Broglie waves of an electron in hydrogen-like atoms, like ordinary standing waves, are reflected from a proton or atomic nucleus. And this happens despite the difference between the stationary  $\psi$ -function of the de Broglie wave of the electron at the center of the quantum resonator from zero in the ground state<sup>[19]</sup>.
- 4) In the case of the collapse of plane de Broglie waves of electrons in hollow quantum resonators, where there are no quantum particles in the center of the resonator (as in the case of polarization capture of electrons by fullerenes ( $C_{60}$ ,  $C_{70}$ ), **Figure 1**), unlimited cumulation of  $\psi_{n-1/2}$  is observed functions of de Broglie waves of electrons to the center of a quantum resonator (**Figure 6b**) and limited cumulation of the probability of finding a particle-wave in the center of a hollow quantum resonator (**Figure 6a**).
- 5) As confirmed experimentally, the collapse of de Broglie waves of electrons, according to the virial theorem, is accompanied by the release of half of the potential energy of the electron, in the case of an atom, in the form of electromagnetic radiation (for a hydrogen atom with energy = 13.61 eV, taking into account the entire cascade of transitions to the lower energy level).
- 6) During e-capture by an atomic nucleus and neutronization of one proton, according to the virial theorem for quantum systems<sup>[21]</sup>, one should expect radiation, for example, in the form of a neutrino (with energy  $\sim 0.85$  MeV, see for more details<sup>[5]</sup>). When a proton is neutronized and its charge is compensated by an electron, the mass and potential energy of the electron is transformed into the mass of a neutron. According to the fundamentals of quantum mechanics, a light electron cannot be in an atomic nucleus, much less in the region or inside a proton.
- 7) Penetration of an electron into an atomic nucleus and then into a proton is possible only with a dynamic bi-cyclonic mass exchange<sup>[5]</sup> between an electron captured by the atomic nucleus and a proton into which this electron is introduced, gaining mass in the process of the polarization e-capture. As experiments show, such a bi-cyclonic mass exchange between an electron and an atomic nucleus is possible in the case of aluminum  $Z = 13$ , i.e., at sizes  $\sim 4 \times 10^{-12}$  m, which can be estimated according to  $r_1 = a_0/Z = 0.53/Z [10^{-10} \text{ m}]$ —the first Bohr orbit of the de Broglie wave of an electron in a hydrogen-like atom with the charge of the atomic nucleus— $Z$ <sup>[19]</sup>.
- 8) The model of bi-cumulation of de Broglie waves of electrons into atomic nuclei proves the ineffectiveness of the debate about cold or hot nuclear fusion<sup>[5]</sup>. In nature, this synthesis is a structural synthesis, where temperature plays an insignificant role. Here, a significant role is played by pressure (density of the number of particles) and the processes of structural bi-cumulation of  $\psi$ -functions of de Broglie waves of electrons into protons and the probability of penetration of an electron, like a de Broglie wave, into a proton in the atomic nucleus. This is possible when the proton is polarized to the captured electron in the form of a mass jet, increasing the effective mass of the electron collapsing into the proton.
- 9) Neutron instability in the meso world ( $\sim 15$  min, which is very stable for the femto world, the next stable state is a million times less) suggests the existence of cumulative-dissipative structures based on neutrinos and antineutrinos, taking part in the resonant collisional destruction of neutrons.
- 10) Gravity leads to the accumulation of enormous mass into galaxies, quantum stars and black holes.

This occurs as a result of the processes of neutronization of matter and is accompanied by the collapse of de Broglie waves of electrons from sizes  $10^{-10}$  m to  $10^{-15}$  m. In this case, the characteristic volume of a quantum star changes by a factor of  $10^{15}$ . The gravitational energy released in this case is hundreds of times higher than the electrical energy<sup>[5]</sup>. In complex cumulative-dissipative interference of Coulomb, gravitational and centrifugal forces occur in cumulative-dissipative structures with sizes from  $10^{-15}$  to  $10^{27}$  m.

### 3. Conclusion

We have obtained original analytical results on the generalization of the model of structural stationary and dynamic limited and unlimited cumulation of de Broglie waves of electrons and electric field for various types of e-capture and neutronization of matter on the characteristic sizes of cumulative-dissipative structures from  $10^{-15}$  m to  $10^{26}$  m<sup>[5]</sup>. When electrons are captured by fullerenes, the partial collapse of the  $\psi$ -function of electrons obeys the general laws of collapse. The discoveries and classification of quantum-size effects of nanometer sizes presented by us will undoubtedly find their application in nanotechnologies for their application in strengthening the world's human potential.

Quantum polarization resonators for de Broglie waves of electrons and self-forming negative endo-ions (with endo-electrons inside them) based on fullerenes and carbon nanotubes have enormous strength (exceeding the strength of diamond). These strength properties make it possible (without destroying endo-ions) to move them in electric fields, to study such structures and determine in experiments and theories: the lifetime of negative endo-ions of fullerenes with electrons inside, the resonance energy of trapped electrons<sup>[7-9]</sup>, the profile of the probability of finding endo-electrons in the cavity fullerene<sup>[5]</sup>, etc. This can be done without significantly modifying their parameters, given that the polarization forces that hold the electron in the endoion are significantly greater than the forces acting on the entire endo-ion. Of particular interest for explaining quantum dualism, based on experiments<sup>[7-9]</sup>, is our classification of processes associated with the movement of a particle (corpuscle) and with wave processes already manifested in the statistical behavior of electrons, see Effect 29.

Studies of Effect 29 have revealed that the electron wave function can be not only in the form of a plane de Broglie wave, but also in the form of a spherically symmetric cos wave, cumulating indefinitely towards the center of the quantum resonator. In principle, the spherical symmetry of the wave functions of de Broglie waves of electrons in atoms has been reported previously. But they were limited to the center of the atom.  $\psi$ -function of electrons in the general case is determined by the symmetry of the Schrödinger equation and correctly set boundary conditions for reflection from other quantum particles and polarization (Coulomb) barriers<sup>[5]</sup>. Hence its connection with the observer and other now understandable paradoxes. If in front is a screen with two slits, then the  $\psi$ -function is a plane wave; if in front is a spherically symmetric fullerene, then the  $\psi$ -function will also be spherically symmetric. Therefore, the  $\psi$ -function describes the behavior of the particle as a wave, and does not make the particle a wave. A particle always remains a corpuscle with a certain charge, mass, etc. (unless it transmutes with a proton to a neutron). The constant release of an electron as a particle from the fullerene leads to constant polarization of the fullerene (**Figure 1** and **6**). Therefore, it is possible to calculate the quality factor of nanometer-sized quantum resonators. The idea that under certain conditions the particles themselves become waves or shells is erroneous! De Broglie's statement about the wave nature of the particle itself is also erroneous. A particle or a large system of them only behaves statistically as waves and this behavior can be described statistically through the Schrödinger equation with the correct boundary conditions. In this case, limiting conditions (such as the Dirac ban) should be imposed not on the  $\psi$ -function, but on the

probability of finding a particle in the volume<sup>[5]</sup>.

The knowledge gained from studying the polarization forces between charged quantum particles and spherically symmetric structures with an electron gas on their surface is easily transferred to their interactions with cylindrically symmetric quantum resonators—nano-tubes<sup>[5]</sup> and other systems of nucleons with electrons. Such studies carried out in experiments<sup>[7–9]</sup> allowed us to:

- 1) Describe in time the process of transformation (limited and unlimited collapse, or reduction according to von Neumann) of the  $\psi$ -function of the de Broglie wave of a free electron when it is captured by a spherically symmetric hollow polarization barrier, see **Figure 1**, for  $C_{60,70}$ .
- 2) Prove that in quantum mechanics there are analogues of cumulative classical wave processes.
- 3) Prove analytically and on the basis of these experimental observations<sup>[7–9]</sup> that Dirac's requirement that the  $\psi$ -function is limited for de Broglie waves everywhere is excessive and can be replaced by the requirement that the probability of finding a particle in any volume is limited and the presence of quantum reflection (rebound) de Broglie waves of electrons with low kinetic energy from atomic nuclei and protons.

Based on experiments<sup>[7–9]</sup>, we have proven, using the energy spectra of captured de Broglie waves of electrons, that in nature it is possible to realize half a de Broglie wave in hollow quantum spherically and cylindrically symmetric resonators (a wave with one antinode and nodes on the boundary  $r=R+r_{ind}$ )<sup>[3,5,6,22,23]</sup>.

The unlimited cumulation of de Broglie waves cannot be described within the framework of the old (Bohr) theory, which involves the orbital model of the hydrogen atom (cos-waves are impossible in it). In the Bohr model, electrons move in orbits rather than converging as waves towards the center of a quantum hollow resonator. **The author provides all the irrefutable evidence of his statement that cumulative quantum mechanics is a logical consequence of Schrödinger's new (wave) quantum mechanics, capable of describing all known cumulative and dissipative phenomena and structures in hollow quantum resonators, both with potential wells and with potential polarization barriers<sup>[5]</sup>.** We have considered the process in time of unlimited and limited collapse and modification of the  $\psi$ -function of quantum particles during their capture in hollow spherically or cylindrically symmetric polarizing quantum resonators (**Figure 6**). It has been shown that phenomena in quantum (wave) mechanics have their analogues in conventional (wave) hydrodynamics of liquids and gases<sup>[5]</sup>.

As a result of the research, the author discovered and classified more than 32 polarization quantum-size effects. This review proves that only by applying the fundamentals of cumulative quantum mechanics can one explain and classify all quantum-size effects discovered by **the author**, based on experiments<sup>[7–9]</sup>. These quantum size effects led to the discovery of the principles of physical doping and the classification of doping into physical and chemical doping. During physical alloying, modification of the properties of a composite is carried out using nano- and microstructures of a foreign material. In this case, fractions of foreign material are not introduced into the crystal lattice. They only decorate the nano- or microcrystals of the supporting material in the composite. Physical doping promotes strengthening of composites by Coulomb compression of physically doped materials, increasing the luminescent properties of phosphors, increasing conductivity up to  $10^{10}$  times and other properties due to quantum-size effects.

**The author will prepare a separate review on the theory of the formation of Vysikaylo's standing excitons of large radius and modification of the properties of nanocomposites during chemical doping of nanostructured materials. To do this, we use cumulative quantum mechanics to describe changes in the**



local dielectric properties of chemically doped materials (diamonds, etc.) and methods for measuring dielectric constant in 0.3 nm steps depending on the distance to the doping atom<sup>[22-30]</sup>.

## Conflict of interest

The author declares no conflict of interest.

## References

1. Vysikaylo PI. Cumulation architecture and reflecting mirrors in structures from femto- to macroscales. Instability of a focusing mass: Collection of works int. Available online: <https://urss.ru/cgi-bin/db.pl?lang=Ru&blang=ru&page=Book&id=106337#FF1> (accessed on 27 January 2024).
2. Vysikaylo PI. Detailed elaboration and general model of the electron treatment of surfaces of charged plasmoids (from atomic nuclei to white dwarves, neutron stars, and galactic cores): Self-condensation (self-constriction) and classification of charged plasma structures—Plasmoids part 1. General analysis of the convective cumulative-dissipative processes caused by the violation of neutrality: Metastable charged plasmoids and plasma lenses. *Surface Engineering and Applied Electrochemistry*. 2012; 48(4): 293-305. doi: 10.3103/S1068375512010164
3. Vysikaylo PI. Cumulative quantum mechanics (CQM) Part II. Application of cumulative quantum mechanics in describing the Vysikaylo polarization quantum-size effects. *Surface Engineering and Applied Electrochemistry*. 2012; 48(5): 395-411.
4. Vysikaylo P, Mitin V, Mashchenko V. Physical Doping Nanocomposites with Carbon Nanostructures with High Electron Affinity. *Sensors & Transducers*. 2021; 248(1): 18-26.
5. Vysikaylo PI. Cumulative quantum mechanics: textbook. Available online: <https://www.elibrary.ru/item.asp?ysclid=lutkbbkbow508233664&edn=apphek> (accessed on 27 January 2024).
6. Vysikaylo PI. Quantum Size Effects Arising from Nanocomposites Physical Doping with Nanostructures Having High Electron Affinit. *Herald of the Bauman Moscow State Technical University Series Natural Sciences*. 2021; 3(96): 150-175. doi: 10.18698/1812-3368-2021-3-150-175
7. Tuktarov RF, Akhmetyanov RF, Shikhovtseva ES. et al. **Plasma oscillations in fullerene molecules during electron capture**. *Journal of ETP Letters*. RF. 2005; 81(4): 207-211. [https://www.mathnet.ru/php/archive.phtml?wshow=paper&jrnid=jetpl&paperid=1679&option\\_lang=eng&ysclid=lwpam7lcwx405769491](https://www.mathnet.ru/php/archive.phtml?wshow=paper&jrnid=jetpl&paperid=1679&option_lang=eng&ysclid=lwpam7lcwx405769491)
8. Jaffke T, Illenbergen E, Lezius M, et al. **Formation of C<sub>60</sub><sup>-</sup> and C<sub>70</sub><sup>-</sup> by free electron capture. Activation energy and effect of the internal energy on lifetime**. *Chem. Phys. Lett*. 1994; 226: 213-218. doi: 10.1016/0009-2614(94)00704-7
9. Huang J, Carman HS, Compton RN. Low-Energy Electron Attachment to C60. *The Journal of Physical Chemistry*. 1995; 99(6): 1719-1726. doi: 10.1021/j100006a013
10. Polyanin AD. Handbook of linear equations of mathematical physics. Available online: <https://al-shell.ru/articles/a-d-polyanin-spravochnik-po-lineynym-uravneniyam-matematicheskoy-fiziki-m-fizmatlit-2001/> (accessed on 27 January 2024).
11. Popov M, Buga S, Vysikaylo P, et al. C60-doping of nanostructured Bi-Sb-Te thermoelectrics. *physica status solidi (a)*. 2011; 208(12): 2783-2789. doi: 10.1002/pssa.201127075
12. Reed CA, Bolskar RD. Discrete Fulleride Anions and Fullerenium Cations. *Chemical Reviews*. 2000; 100(3): 1075-1120. doi: 10.1021/cr980017o
13. Sidorov LN, Yurovskaya MA, Borshchevsky AY, et al. Fullerenes: textbook. Available online: [https://vk.com/wall-70921366\\_34374](https://vk.com/wall-70921366_34374) (accessed on 27 January 2024).
14. Vysikaylo PI. Cumulative Point—L<sub>1</sub> Between Two Positively Charged Plasma Structures (3-D Strata). *IEEE Transactions on Plasma Science*. 2014; 42(12): 3931-3935. doi: 10.1109/tps.2014.2365438
15. Popova DM, Mavrin BN, Denisov VN, et al. Spectroscopic and first-principles studies of boron-doped diamond: Raman polarizability and local vibrational bands. *Diamond and Related Materials*. 2009; 18(5-8): 850-853. doi: 10.1016/j.diamond.2009.01.028
16. Casimir HBG. On the attraction between two perfectly conducting plates. *Proc. Kon. Nederl. Akad. Wet.* 1948; 51: 793.
17. Vysikaylo PI. Peripheral coulomb forces, classical and quantum membranes, focusing plasmoids (review). *Successes in applied physics*. 2015; 3(5): 471-478.
18. Vysikaylo PI. Cumulative physics of crystals and plasmoids. *Successes in applied physics*. 2015; 3(3): 226-235.
19. Landau LD, Lifshits EM. *Theoretical physics: textbook*. allowance. Available online:



- <https://archive.org/details/Teor-fizika-10-tomov-3-tom-2004> (accessed on 27 January 2024).
20. Zababakhin EI, Zababakhin IE. Phenomena of unlimited cumulation. Available online: <https://rusist.info/book/5707267?ysclid=luzdgpfs48922313383> (accessed on 27 January 2024).
  21. Fock V. Note on the virial set (German). *Zeitschrift für Physik A*. 1930; 63(11): 855-858. doi: 10.1007/BF01339281
  22. Vysikaylo PI. Self-organizing cumulatively dissipative nanostructures in doped crystals. Paradoxes in quantum mechanics and their solution based on cumulative quantum mechanics. *Engineering physics*. 2013; (3): 15-48.
  23. Vysikaylo PI. Capture of electrons into hollow polarizing carbon molecules in nanocomposites. Analytical description of the emission spectra of standing excitons in crystals of the iv group of elements doped with AS, B, P. *News of higher educational institutions. Series: Chemistry and Chemical Technology*. 2013; 56(7): 71-75.
  24. Vysikaylo PI, Belyev VV. Methodology for experimentally calculated determination of the profile and local values of the relative dielectric constant of acceptor-doped crystals from Raman spectra. [https://www.vniims.ru/download/doc/gssssd/Perechen\\_metodik\\_GSSSD.pdf?ysclid=lwp9y2pwx329415948](https://www.vniims.ru/download/doc/gssssd/Perechen_metodik_GSSSD.pdf?ysclid=lwp9y2pwx329415948) № is in order 186. 02.12.2016. Moscow № 249a -2016. 33p.
  25. Vysikaylo PI. Nano-oscillations in the profiles of relative dielectric permitibilities in doped crystals. *Electronic engineering. Series 3 Microelectronics. Scientific & Technical Journal*. 2019; 4(176): 2-20.
  26. Denisov VN, Mavrin BN, Polyakov SN, et al. First observation of electronic structure of the even parity boron acceptor states in diamond. *Physics Letters A*. 2012; 376(44): 2812-2815. doi: 10.1016/j.physleta.2012.08.033
  27. Collins AT, Williams AWS. The nature of the acceptor centre in semiconducting diamond. *J. Phys. C: Solid State Phys*. 1971; 4: 1789-1800. doi: 10.1088/0022-3719/4/13/030
  28. Cherenko RM. Boron, the Dominant Acceptor in Semiconducting Diamond. *Phys. Rev. B*. 1973; 7: 4560-4567. doi: 10.1103/PhysRevB.7.4560
  29. Collins AT, Lightowers EC, Dean PJ. Role of Phonons in the Oscillatory Photoconductivity Spectrum of Semiconducting Diamond. *Phys. Review*. 1969; 183(3): 725-730. doi: 10.1103/PhysRev.183.725
  30. Polyakov SN, Denisov VN, Mavrin BN, et al. Formation of Boron-Carbon Nanosheets and Bilayers in Boron-Doped Diamond: Origin of Metallicity and Superconductivity. *Nanoscale Res Lett*. 2016; 11(11). doi: 10.1186/s11671-015-1215-6